Supporting Information for

Complex of Poly(4-vinylpyridine) and Tolane Based Hemi-phasmid Benzoic Acid: Towards Luminescent Supramolecular Side-Chain Liquid Crystalline Polymer

Shao-Jie Wang, Rui-Ying Zhao, Shuang Yang, Zhen-Qiang Yu, Er-Qiang Chen

Table of Contents

Materials and Instruments

Poly(4-vinylpyridine) (P4VP) [weight average molecular weight (M_w) of 6×10^4 g/mol] was purchased from Sigma-Aldrich, which was dried in vacuum at 60 °C for 2 days prior to use. Methyl 4-iodobenzoate, (trimethylsilyl)acetylene, and 4-iodophenol were purchased from Sigma-Aldrich. Tetrahydrofuran (THF) was distilled under normal pressure from CaH_2 immediately prior to use. Triethylamine was distilled and dried over KOH. All the other chemicals obtained from Beijing Chemical Co. were analytical grade and used as received.

^{1}H NMR and ^{13}C NMR spectra were recorded on a Bruker ARX400 spectrometer in $CDCl_3$ solutions (400 and 100 MHz for ^{1}H NMR and ^{13}C NMR, respectively). Chemical shifts of ^{1}H and ^{13}C NMR were quoted to internal standard $(CH_3)_4Si$. Mass spectra were recorded on a Bruker APEX IV mass spectrometer. Elemental analyses were performed using a German Vario EL III elemental analyzer.

Infrared spectra (IR) were recorded using a Bruker VECTOR22 FT-IR spectrometer. Samples were prepared by casting one drop of the chloroform solution (~10 mg/mL) directly on potassium bromide crystals. After sample drying, the FT-IR measurements were taken at room temperature.

Differential scanning calorimetry (DSC) experiments were carried out using PerkinElmer Pyris I DSC with a mechanical refrigerator. The temperature and heat flow were calibrated using standard materials such as benzoic acid and indium. The dried samples were encapsulated in a sealed aluminum pan with the sample weight of ~5 mg. All the samples were first melted at 155 °C for 3 min to erase the thermal history and then cooled to -10 °C at a rate of 1 °C/min. The subsequent DSC heating traces (form -10 to 160 °C) were recorded with a rate of 20 °C/min.

The birefringence and liquid crystalline texture of samples were examined under a polarized optical microscopy (POM, Leica DML) with a Mettler hot stage (FP-90). The samples were prepared by melting the dried samples sandwiched between a glass slide and a cover glass. After being annealed 30 min at 130 °C, the samples were cooled to room temperature at a rate of 0.5 °C/min.

The phase structures of samples were investigated using X-ray diffraction (XRD). One-dimensional (1D) XRD experiments were mainly performed with the high-flux small-angle X-ray scattering instrument (SAXSess, Anton Paar) equipped with a Kratky block collimation system and a

Philips PW3830 sealed-tube X-ray generator (Cu Kα). The small-angle and wide-angle X-ray scattering patterns of the samples can be simultaneously recorded on an imaging plate with a pixel size of 42.3×42.3 μm^2 which extends to the high-angle range (the q-range covered by the imaging plate is from 0.06 to 29 nm^{-1}, $q = 4\pi\sin\theta/\lambda$, where λ is the wavelength of 0.1542 nm and 2θ the scattering angle). The scattering peak positions were calibrated with silver behenate. The original experimental data such as data acquisition, background subtraction, and data reduction were handled by Anton Paar SAXSquant 1.01 software and PCG software package. Before measurement, the samples of P4VP(**1**)$_x$ were further annealed at 120 °C for 15 min followed by cooling to room temperature at a rate of 0.5 °C/min. A temperature control unit (Anton Paar TCS300) in conjunction with the SAXSess was utilized to study the structure evolution as a function of temperature.

Two-dimensional (2D) XRD of the oriented samples was recorded on a Bruker D8 Discover diffractometer with GADDS as 2D detector calibrated with silicon powder ($2\theta > 15°$) and silver behenate ($2\theta < 10°$). The low-angle 2D XRD experiments were carried out on the Nanostar U small-angle X-ray scattering instrument (Bruker AXS) equipped with 3 pinholes collimation system. The X-ray was generated using IμS micro Focus X-Ray source incorporating a 30 W sealed-tube X-ray generator with Cu target. The wavelength is 0.1542 nm. The power of the generator used for measurement was 40 kV and 650 μA. The diffraction patterns were recorded on a Hi-Star 2D detector system with a pixel size of 100×100 μm^2. The distance from the sample to detector was 1059 mm. The spot size of the beam was 1 mm. The exposure time was 60 s. The 2D XRD patterns were obtained through a transmission mode, with the X-ray incident beam aligned either perpendicular or parallel to the shear direction. The background scattering was recorded and subtracted. To performed 2D XRD experiments, the macroscopically oriented samples were prepared by mechanical shearing the sample on a solid substrate at temperatures between 130 and 150 °C, followed by quenching to room temperature.

UV-Vis absorption spectra were recorded on a Hitachi U-4100 spectrophotometer using 1 cm quartz cuvettes. Photoluminescence (PL) spectra were measured on a Hitachi F4500 fluorescence spectrometer in the right-angle geometry and using 1 cm quartz cuvettes. The excitation light was fixed at a wavelength of λ_{ex} = 355 nm and the slits width of 5 nm were used for both

monochromators. The quantum yield (Φ) values were determined using an integrating sphere on a Nanolog FL3-2iHR infrared fluorescence spectroscopy equipped with R928 photomultiplier as detector.

Synthesis of 4-((4-((3,4,5-tris(dodecyloxy)benzyl)oxy)phenyl)ethynyl) benzoic acid (1)

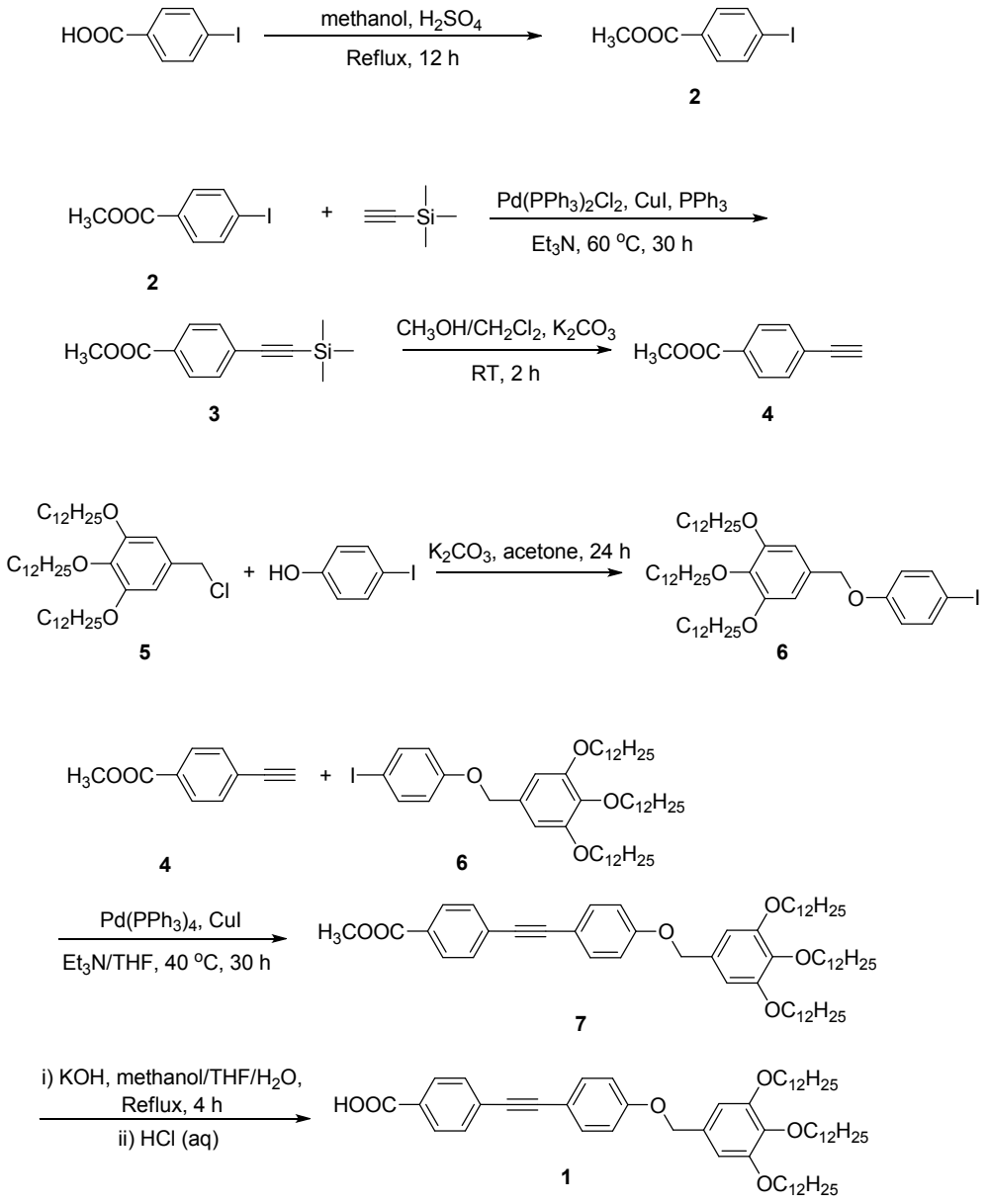

Scheme S1. Synthetic route of compound **1**.

Methyl 4-((trimethylsilyl)ethynyl)benzoate (3). Compound **3** was synthesized according to literatures.[1-4] Compound **2** (3.00 g, 11.4 mmol), bis(triphenylphosphine)palladium(II) dichloride (80.2 mg, 0.114 mmol), triphenylphosphine (59.8 mg, 0.228 mmol), copper(I) iodide (21.7 mg, 0.114 mmol), dried triethylamine (30 mL) were added into one two-necked round-bottom flask under

nitrogen. Trimethylsilylacetylene (3.50 mL, 22.7 mmol) was injected after the mixture being stirred at room temperature for 5 minutes. After reacted at 60 °C for 30 hours, the formed precipitate was removed by filtration and washed with diethyl ether. The crude product was condensed and purified on a silica-gel column using hexane/ethyl acetate (volume ratio 80/1) as the eluent. A white solid was obtained in 96% yield. ^{1}H NMR (ppm, $CDCl_3$): δ 0.27 (s, 9H), 3.91 (s, 3H), 7.51 (d, J = 8.7 Hz, 2H), 7.96 (d, J = 8.3 Hz, 2H). ^{13}C NMR (ppm, $CDCl_3$): δ 0.0, 52.1, 97.6, 104.0, 127.7, 129.3, 129.6, 131.8, 166.4. HRMS (ESI): Calcd for *m/z* [MH^+]: 233.0992; Found *m/z* [MH^+]: 233.0991. Elemental analysis (EA, %): Calcd C, 67.20; H, 6.94; O, 13.77; Si, 12.09; Found C, 67.21; H, 6.94; O, 13.76; Si, 12.09.

Methyl 4-ethynylbenzoate (4). Compound **3** (1.00 g, 4.32 mmol) was dissolved in methanol (30 mL) and the cosolvent dichloromethane (30 mL), and then potassium carbonate (2.98 g, 21.6 mmol) was added. The mixture was stirred at room temperature for 2 h and then added to water (50 mL) to quench the reaction. The mixture was extracted with dichloromethane (2 × 50 mL), and then the combined organic extracts were then dried over anhydrous $NaSO_4$ and filtered. The solvent was evaporated in vacuo to afford the desired product **4** (0.66 g, 96%) as brown crystals that was immediately reacted in the next step without further purification. ^{1}H NMR (ppm, $CDCl_3$): δ 3.24 (s, 1H), 3.92 (s, 3H), 7.55 (d, J = 8.4 Hz, 2H), 7.99 (d, J = 8.4 Hz, 2H). ^{13}C NMR (ppm, $CDCl_3$): δ 0.0, 52.3, 76.7, 77.0, 77.4, 80.1, 82.8, 126.8, 129.5, 130.1, 132.1, 166.3. HRMS (ESI): Calcd for *m/z* [MH^+]: 161.0597; Found *m/z* [MH^+]: 161.0593. Elemental analysis (EA, %): Calcd C, 74.99; H, 5.03; O, 19.98; Si, 12.09; Found C, 75.00; H, 5.03; O, 19.97.

1,2,3-tris(dodecyloxy)-5-((4-iodophenoxy)methyl)benzene (6). To a solution of **5**[5] (6.79 g, 10.0 mmol) in dry acetone (100 mL), 4-iodophenol (3.30 g, 15.0 mmol) was added followed by K_2CO_3 (6.90 g, 50.0 mmol) and reaction mixture was refluxed for 24 hours. Then the precipitate formed was filtered and washed with dichloromethane. The organic fractions were combined and the solvent was evaporated in vacuo. The pale yellow solid thus obtained was then purified on a silica-gel column using hexane/ethyl acetate (volume ratio 80/1) as the eluent. A white solid was obtained in 93% yield. ^{1}H NMR (ppm, $CDCl_3$): δ 0.85-0.90 (t. J(H,H) = 6.8 Hz, 9H), 1.20-1.40 (m, 48H), 1.40-1.48 (m, 6H), 1.65-1.82 (m, 6H), 3.90-3.98 (m, 6H), 4.90 (s, 2H), 6.58 (s, 2H), 6.74 (d, J = 8.8

Hz, 2H), 7.55 (d, J = 8.8 Hz, 2H). ^{13}C NMR (ppm, $CDCl_3$): δ 0.0, 14.1, 22.7, 26.1, 29.4, 29.6, 29.7, 30.4, 32.0, 69.2, 70.5, 73.5, 76.7, 77.0, 77.2, 77.3, 83.1, 106.1, 117.3, 131.3, 138.1, 138.2, 153.4, 158.7. HRMS(ESI): Calcd for *m/z* [MH^+]: 880.5674; Found *m/z* [MH^+]: 880.5659. Elemental analysis (EA, %): Calcd C, 68.19; H, 9.69; O, 7.41; I, 14.70.; Found C, 68.20; H, 9.69; O, 7.41; I, 14.69.

Methyl 4-((4-((3,4,5-tris(dodecyloxy)benzyl)oxy)phenyl)ethynyl)benzoate (7). Compound **6** (1.08 g, 1.25 mmol), tetrakis(triphenylphosphine)palladium (46.0 mg, 0.035 mmol), copper(I) iodide (7.1 mg, 0.038 mmol) were added into one two-necked round-bottom flask under nitrogen. Then the solution of **4** (0.200 g, 1.25 mmol) in 30 mL dried triethylamine/THF (volume ratio 2/1) was bumped with nitrogen for 5 minutes and injected into the flask immediately. A transparent yellow solution was obtained and some white precipitate was formed after a few minutes. After reacted at 40 °C for 30 hours, the formed precipitate was removed by filtration and washed with diethyl ether. The crude product was condensed and purified on a silica-gel column using hexane/dichloromethane (volume ratio 8/1) as the eluent. A yellow solid was obtained in 90.0% yield. ^{1}H NMR (ppm, $CDCl_3$): δ 0.85-0.90 (t. J(H,H) = 6.8 Hz, 9H), 1.20-1.40 (m, 48H), 1.40-1.50 (m, 6H), 1.70-1.82 (m, 6H), 3.92 (s, 3H), 3.93-4.00 (m, 6H), 4.97 (s, 2H), 6.61 (s, 2H), 6.96 (d, J = 8.8 Hz, 2H), 7.48 (d, J = 8.8 Hz, 2H), 7.56 (d, J = 8.4 Hz, 2H), 8.01 (d, J = 8.4 Hz, 2H), . ^{13}C NMR (ppm, $CDCl_3$): δ 0.0,14.1, 22.7, 26.1, 29.4, 29.6, 29.7, 30.4, 31.9, 52.1, 69.2, 70.5, 73.5, 76.7, 77.0, 77.3, 87.6, 92.5, 106.2, 115.0, 115.1, 128.4, 129.2, 129.5, 131.3, 131.4, 133.3, 138.2, 153.4, 159.2, 166.6. HRMS (ESI): Calcd for *m/z* [MH^+]: 895.6810; Found *m/z* [MH^+]: 895.6779. Elemental analysis (EA, %): Calcd C, 79.15; H, 10.13; O, 10.72.; Found C, 79.16; H, 10.15; O, 10.70.

4-((4-((3,4,5-tris(dodecyloxy)benzyl)oxy)phenyl)ethynyl)benzoic acid (1). To a solution of **7** (1.00 g, 1.12 mmol) in methanol/THF/H_2O (50 mL/5 mL/1 mL), KOH (0.63 g, 11.2 mmol) was added and the reaction mixture was stirred under ice-bath till KOH solved completely. After refluxed for 4 hours, the solvent was evaporated in vacuo. The residue was resolved in 30 mL THF and following 3M HCl was added to make sure the pH of the solution arrived at 3 ~ 4. Then the mixture was extracted with diethyl ether (3 × 50 mL), and then the combined organic extracts were then dried over anhydrous Na_2SO_4 and filtered. The solvent was evaporated in vacuo to afford the desired

product **1** (0.88 g, 90%) as brown crystals. A white solid was obtained after recrystallization with ethanol in 85% yield. ^{1}H NMR (ppm, $CDCl_3$): δ 0.86-0.90 (t. J(H,H) = 6.4 Hz, 9H), 1.20-1.40 (m, 48H), 1.40-1.50 (m, 6H), 1.70-1.82 (m, 6H), 3.93-4.00 (m, 6H), 4.98 (s, 2H), 6.61 (s, 2H), 6.96 (d, J = 8.8 Hz, 2H), 7.50 (d, J = 8.8 Hz, 2H), 7.59 (d, J = 8.4 Hz, 2H), 8.08 (d, J = 8.4 Hz, 2H), . ^{13}C NMR (ppm, $CDCl_3$): δ 0.0, 14.1, 22.7, 26.1, 26.2, 29.4, 29.5, 29.6, 29.7, 29.8, 30.4, 32.0, 69.2, 70.5, 73.5, 76.7, 77.0, 77.2, 77.3, 87.6, 93.1, 106.2, 115.0, 115.1, 128.2, 129.3, 130.1, 131.4, 133.3, 138.1, 153.4, 159.3, 171.2. HRMS (ESI): Calcd for *m/z* [MNa^+]: 903.6473; Found *m/z* [MNa^+]: 903.6475. Elemental analysis (EA, %): Calcd C, 79.04; H, 10.06; O, 10.89.; Found C, 79.04; H, 10.06; O, 10.89.

Preparation of the Complex of P4VP(1)$_x$

P4VP(**1**)$_x$ (*x* denotes the molar ratio of **1** to the repeat unit of P4VP) was prepared from chloroform solution unless otherwise stated. In each case, **1** and chloroform were first mixed together until a clear solution was obtained. P4VP was subsequently added, followed by mechanical stirring for about 12 hours at room temperature. The concentrations were kept low (~10 mg/mL) to ensure homogeneous complex formation. Then the solution was dropped at the PTFE plate. After the solvent was evaporated, the complex samples were further dried at 60 °C in vacuum at least for 2 days and thereafter stored in desiccator.

NMR Spectra of Each Compound Synthesized

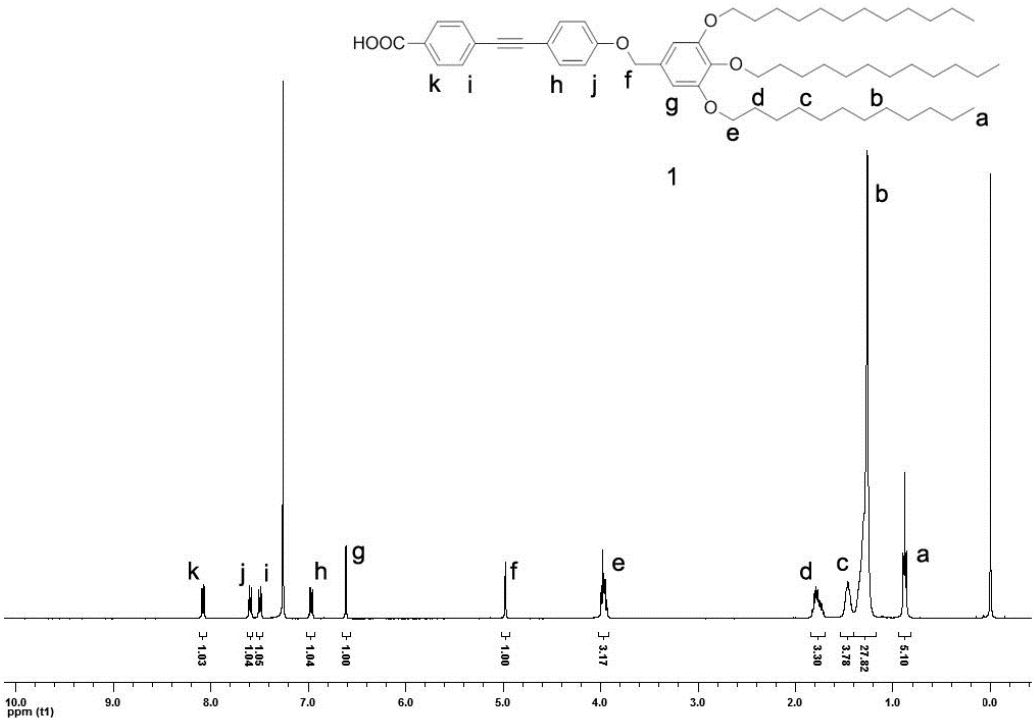

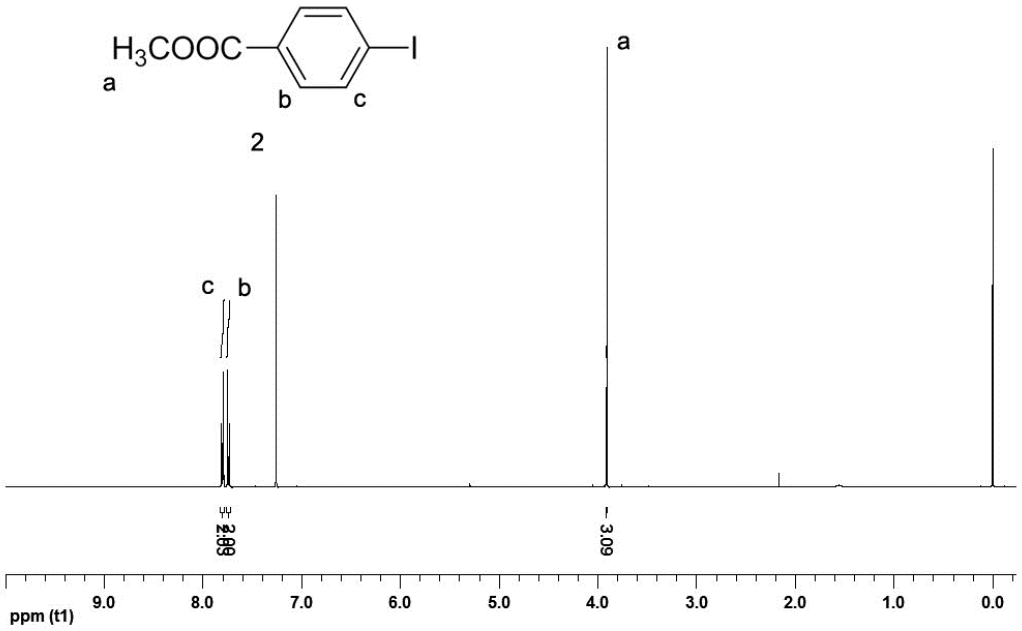

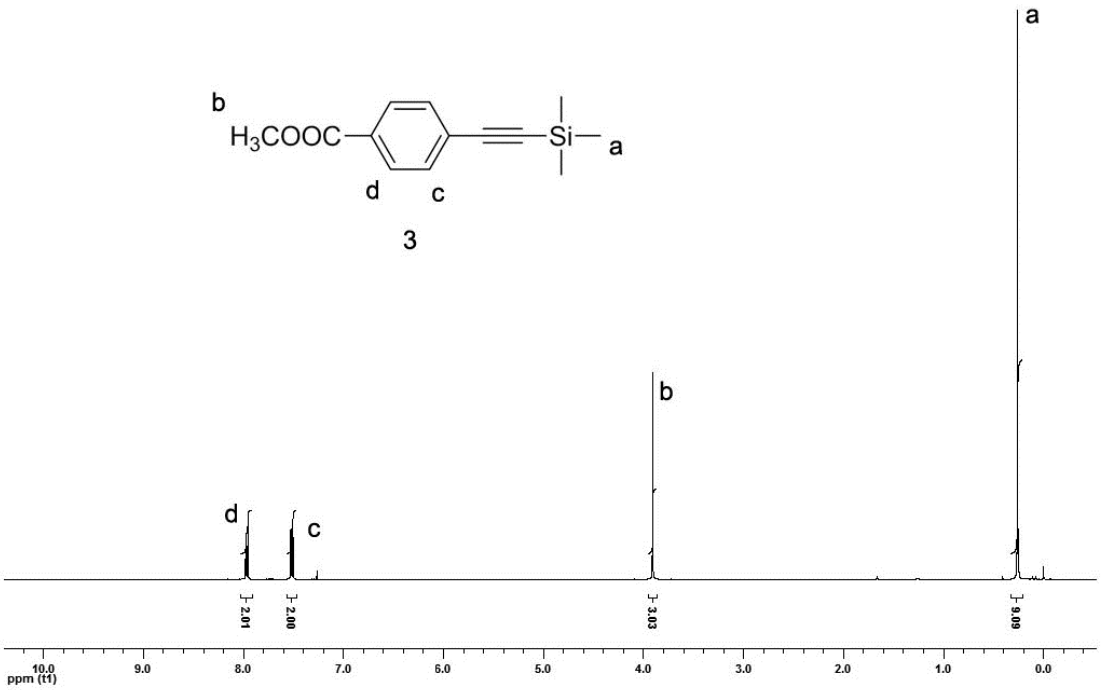
b
H3COOC
Si
a
d
c
3
a
b
d
c
2.01
2.00
3.03
9.09
10.0
9.0
8.0
7.0
6.0
5.0
4.0
3.0
2.0
1.0
0.0
ppm (t1)

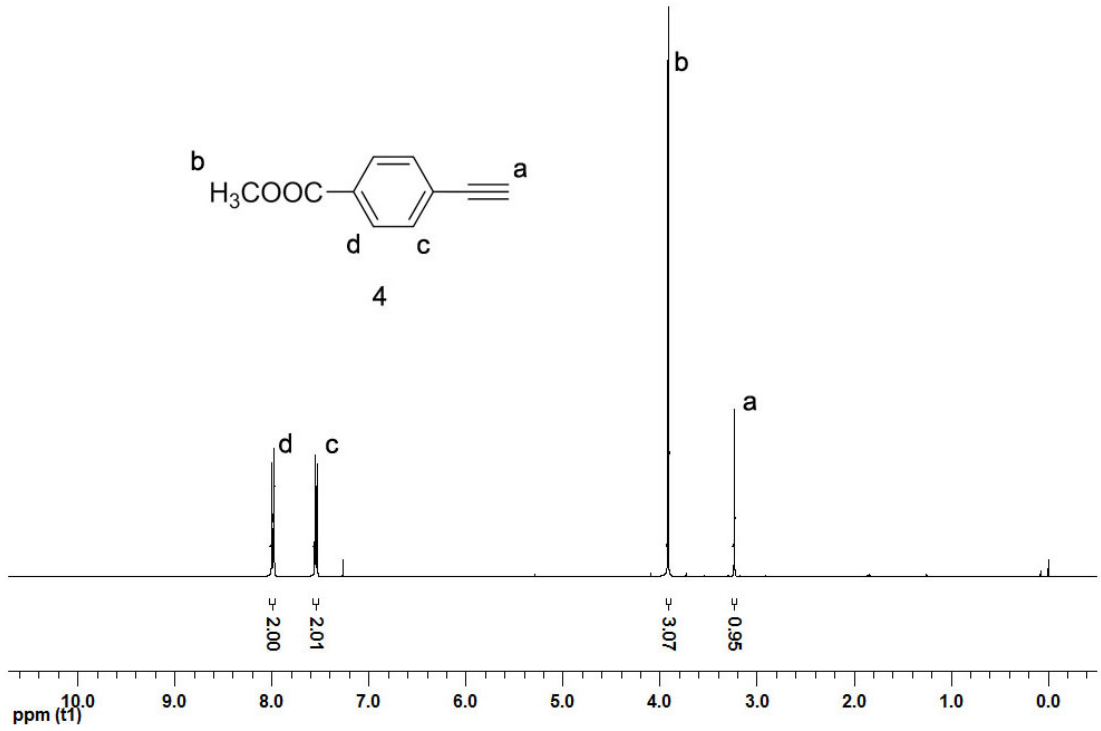
b
H3COOC
a
d
c
4
b
a
d
c
2.00
2.01
3.07
0.95
10.0
9.0
8.0
7.0
6.0
5.0
4.0
3.0
2.0
1.0
0.0
ppm (t1)

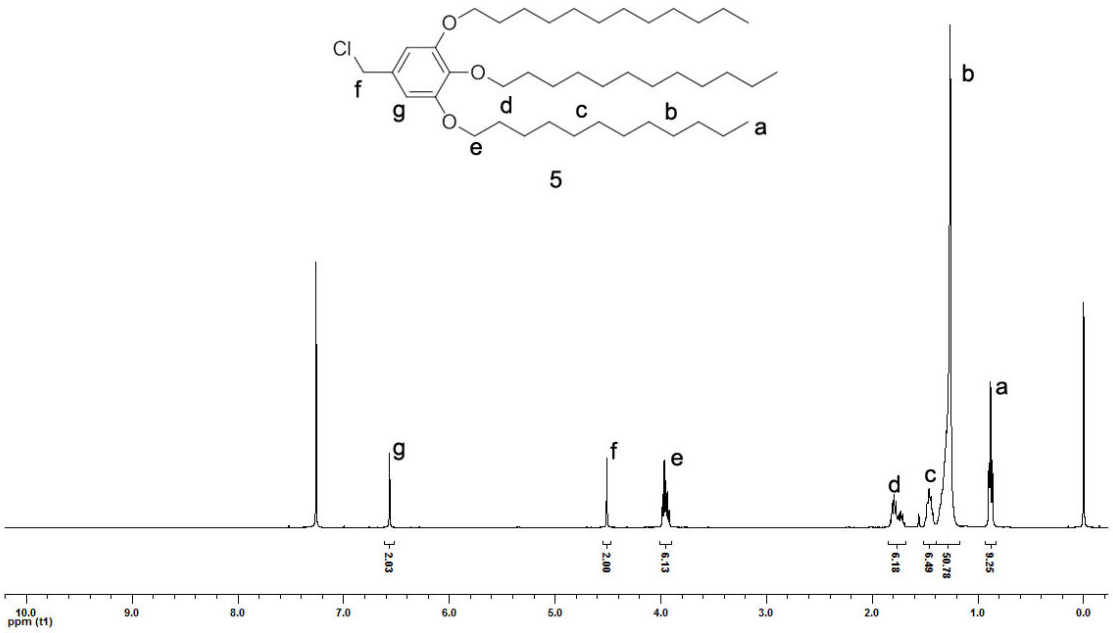
Cl
O
O
O
f
g
d
c
b
a
e
5
b
a
g
f
e
d
c
2.03
2.00
6.13
6.18
6.49
50.78
9.25
10.0
ppm (t1)
9.0
8.0
7.0
6.0
5.0
4.0
3.0
2.0
1.0
0.0

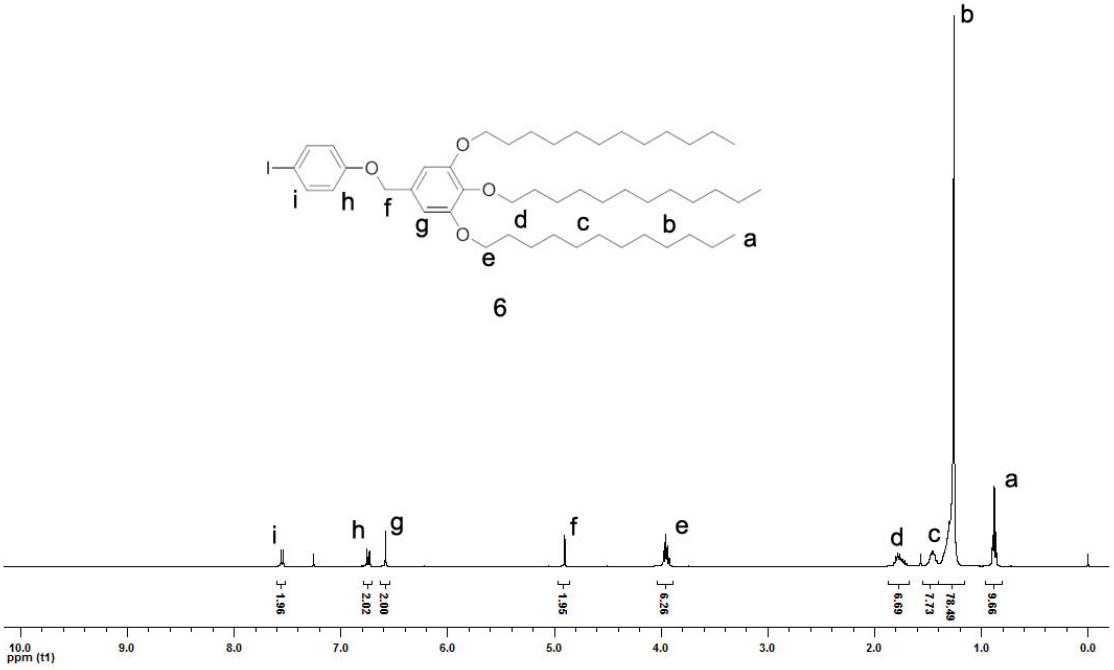
I
O
O
O
i
h
f
g
d
c
b
a
e
6
b
a
i
h
g
f
e
d
c
1.96
2.02
2.00
1.95
6.26
6.69
7.73
78.49
9.66
10.0
ppm (t1)
9.0
8.0
7.0
6.0
5.0
4.0
3.0
2.0
1.0
0.0

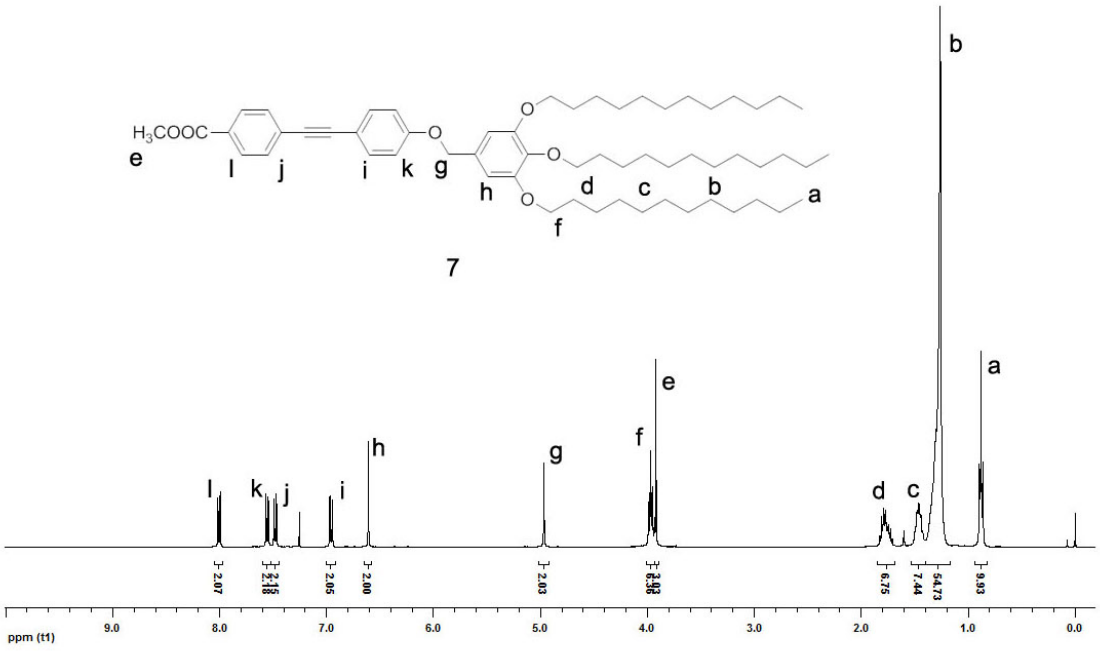
H3COOC
e
l
j
i
k
g
h
d
c
b
a
f
O
7
b
a
e
f
h
g
l
k
j
i
d
c
2.07
2.15
2.18
2.05
2.00
2.03
6.75
7.44
64.73
9.93
ppm (t1)
9.0
8.0
7.0
6.0
5.0
4.0
3.0
2.0
1.0
0.0

DSC and XRD Data of Compound 1

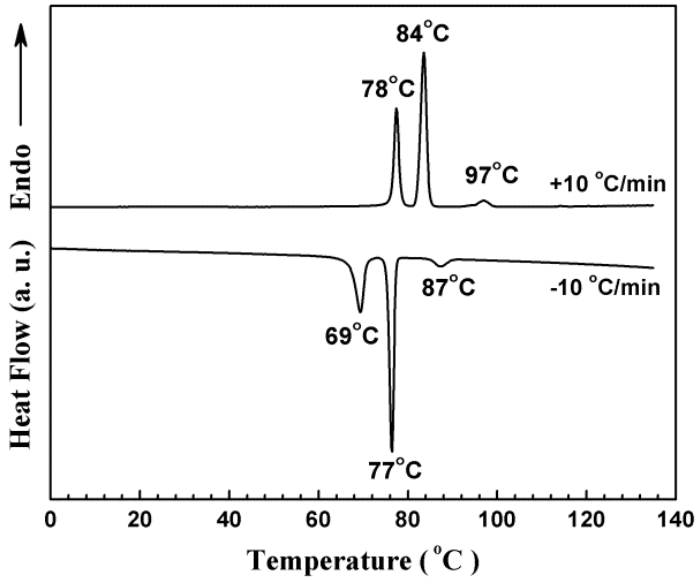

Figure S1. DSC traces of compound **1** recorded during the cooling and subsequent heating processes at a rate of 10 °C/min. The enthalpies (temperatures) of the three phase transitions detected upon heating are 11.82 kJ/mol (78 °C), 20.72 kJ/mol (84 °C) and 1.43 kJ/mol (97 °C), respectively.

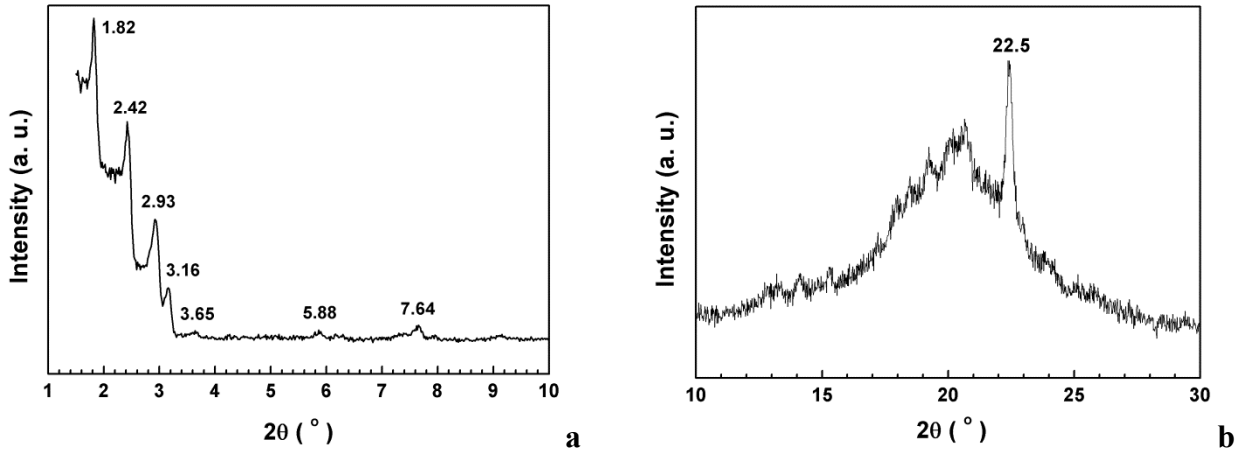

Figure S2. 1D XRD profile of compound **1** at room temperature. The sample was first heated to the isotropic phase, then cooled to room temperature slowly at the rate of 0.5 °C/min. (a) Several sharp and strong diffraction peaks are observed in the low-angle region (2θ of 1.5 ~ 4.0°). (b) In the high-angle region, the sharp diffraction peak at the 2θ of ~22.5° corresponds to a *d*-spacing of 0.39 nm, which should be the π-π stacking distance between two neighboring tolane groups.

DSC Traces of P4VP(1)$_x$ with Various x

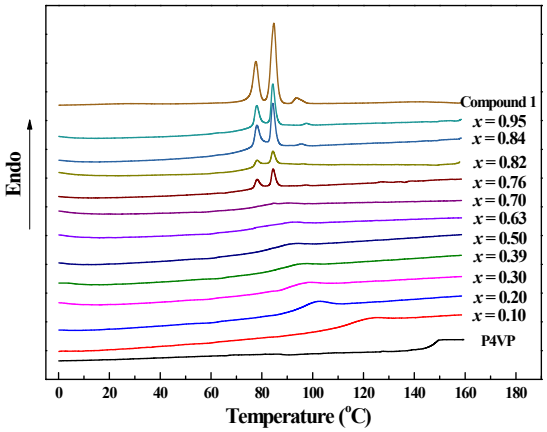

Figure S3. DSC traces of P4VP(**1**)$_x$ recorded during the second heating at a rate of 20 °C/min. For P4VP(**1**)$_x$ with $x \leq 0.70$, only glass transition was detected by DSC, and the glass transition temperature (T_g) decreases with increasing x. When x excessed 0.70, DSC heating traces of the samples also show the phase transition peaks of the pure **1**. In the DSC experiments, since at above 160 °C molecule **1** would be damaged easily, the samples were first heated to 155 °C, where is higher than the glass transition temperature of the complexes, and annealed 3 mins to erase the thermal history. In order to visualize the glass transition more clearly, the samples were then slowly cooled to -10 °C at a rate of 1 °C/min followed by a relatively fast heating at a rate of 20 °C. We also checked the cooling traces recorded with different rates, and confirmed that except the samples with $x > 0.7$ only the glass transition could be detected.

FT-IR Result of P4VP(1)$_x$

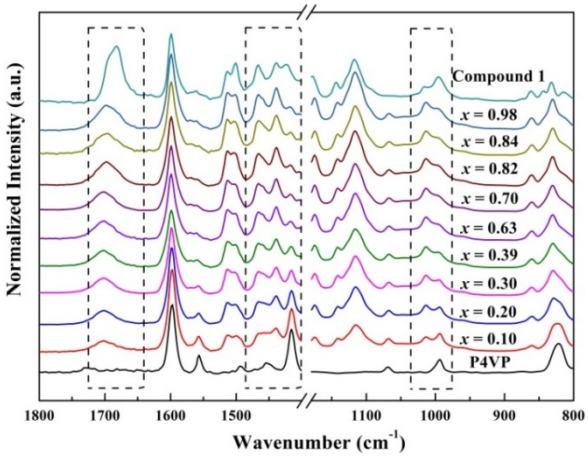

Figure S4. FT-IR spectra of P4VP(**1**)$_x$ with various x recorded at room temperature. For comparison, the spectra of pure P4VP and compound **1** are also shown. The dashed boxes in the figure highlight the differences among P4VP, P4VP(**1**)$_x$, and compound **1**. For example, after complexed with P4VP, the absorption peak corresponding to the stretched resonance of carboxyl group, which is at 1690 cm^{-1} for the pure **1**, shifted to a higher wavenumber (~1706 cm^{-1}). The FT-IR result indicates that the

intermolecular hydrogen bonding between P4VP and **1** is formed in P4VP(**1**)$_x$.

1D XRD Profiles of P4VP(1)$_x$

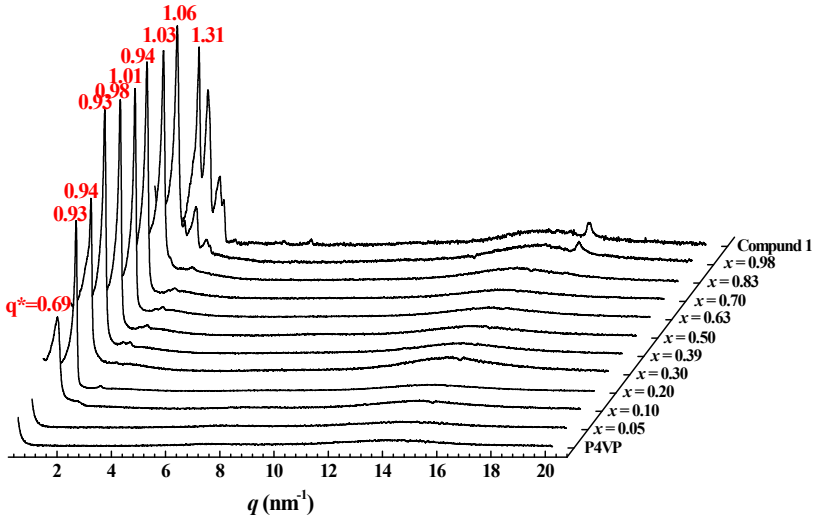

Figure S5. Set of 1D XRD profiles of P4VP(**1**)$_x$ with various x. Both the low- and high-angle regions are shown in the same figure. For comparison, the XRD result of the pure P4VP and **1** are included. At $x > 0.70$, the diffraction of the crystalline **1** can be revealed, which become more clearly with increasing x. For $x \leq 0.70$, only an amorphous halo is observed in the high-angle region.

POM Pictures of P4VP(1)$_x$

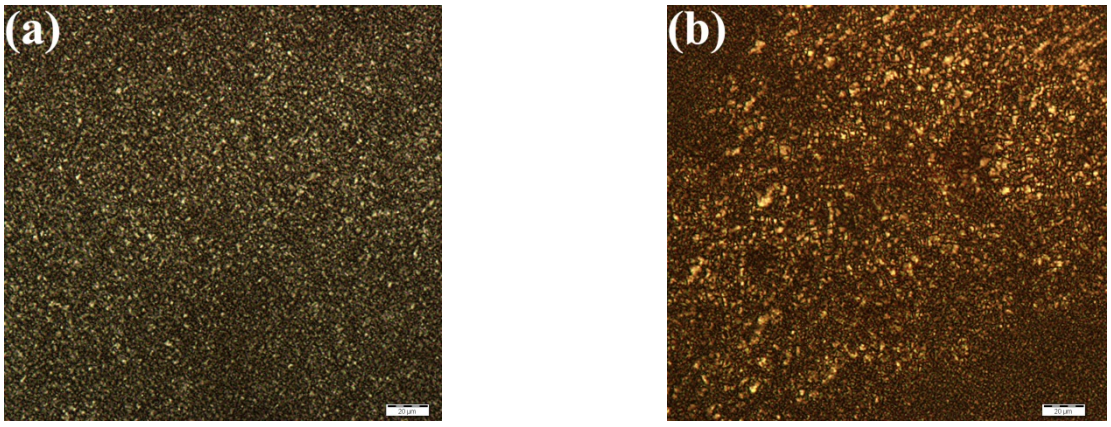

Figure S6. POM pictures of P4VP(**1**)$_{0.15}$ (a) and P4VP(**1**)$_{0.45}$ (b) obtained at room temperature. The scaling bar corresponds to 20 μm. The birefringence and texture observed indicate the liquid crystalline phase formed in the complexes.

_d_-spacings of the First Order Diffraction of P4VP(1)$_x$

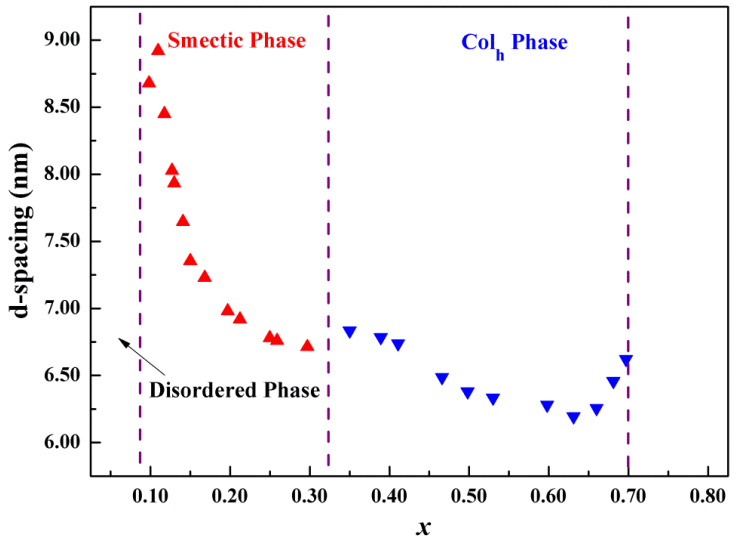

Figure S7. *d*-spacing of the first order diffraction peak in the low-angle region as a function of *x* for P4VP(**1**)$_x$.

Estimation of Domain Size in Liquid Crystalline Structrues of P4VP(1)$_x$

For the liquid crystalline phase of P4VP(**1**)$_x$, we consider that the microphase separation model proposed by ten Brinke and Ikkala et al.[6] is valid. Namely, two sublayers composed of P4VP and **1**, respectively, exist in the smectic (Sm) phase. For the columnar hexagonal (Col$_h$) phase formed at the relatively larger *x*, the P4VP cylinders are embedded in the matrix of **1** with a hexagonal symmetry. Assuming the interface between the P4VP and **1** domains is clear, we can estimate the domain size based on a simple volumetric argument.

We assume that the domain of P4VP possesses the density of ~1.2 g/cm^3, which is close to the density of the pure P4VP. On the other hand, considering that the close packing of **1** molecules in crystalline state cannot be achieved in the complex, the domain of **1** may have a relatively low density of ~1.0 g/cm^3. Therefore, the volume fractions of P4VP and **1** in P4VP(**1**)$_x$, f_{P4VP} and f_1, can be calculated:

$$f_{P4VP} = \frac{\frac{105}{1.2}}{\frac{105}{1.2} + \frac{881x}{1.0}} \qquad (1)$$

$$f_1 = \frac{\frac{881x}{1.0}}{\frac{105}{1.2} + \frac{881x}{1.0}} \qquad (2)$$

wherein the values of 105 and 881 are the molar mass of the repeating unit of P4VP and molecule **1**, respectively. Eq. (1) and (2) can be reduced to:

$$f_{P4VP} = 88/(88 + 881x) \qquad (3)$$

$$f_1 = 881x/(88 + 881x) \qquad (4)$$

With the XRD data available, the thicknesses of sublayer of P4VP and **1** (L_p and L_1) in the Sm phase can be estimated as: $L_p = f_{P4VP}L$ and $L_1 = f_1L$, where L is the layer spacing of the Sm phase. For the Col_h phase of P4VP(**1**)$_x$, the diameter of P4VP cylinder (d_{P4VP}) is estimated as: $d_{P4VP} = (4a^2\sin 60° f_{P4VP}/\pi)^{1/2}$, where a is the lattice parameter of the Col_h phase.

2D XRD Pattern of Oriented P4VP(1)$_{0.15}$ with Sm Phase

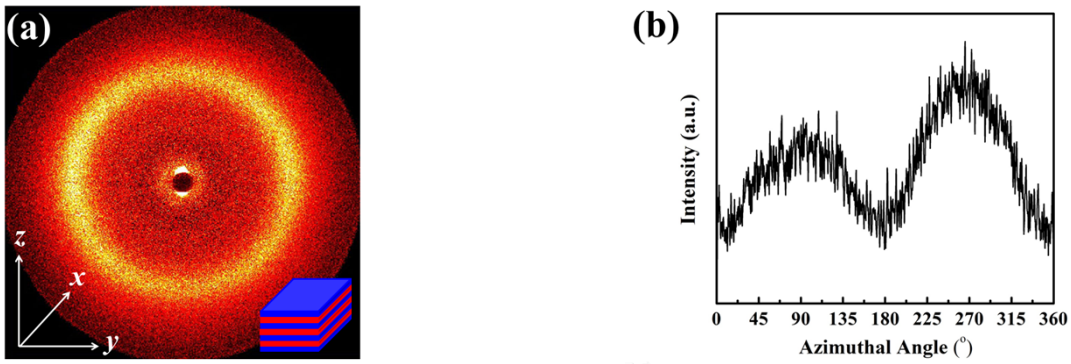

Figure S8. (a) 2D XRD patterns of P4VP(**1**)$_{0.15}$ recorded using Bruker D8 Discover with the X-ray incident beam parallel to the shear direction. The sample was oriented by mechanical shearing. The *x*- and *z*-direction shown in the figure represent the shear direction and shear gradient, respectively. One pair of diffraction arcs at $2\theta = 2.54°$ (close to the beam stop, *d*-spacing of 3.46 nm) appears on the meridian, which corresponds to the second order diffraction of the Sm phase. This confirms that the Sm layer normal is along the *z*-direction. (b) Azimuthal profile of the high-angle scattering located in 2θ range of 14~25°, which indicates that the scattering intensity is more concentrated on the equator, i.e., at the azimuthal angles of 90° and 270°. This observation suggests that the Sm phase should be a smectic A with the rodlike mesogens preferentially parallel to the Sm layer normal.

2D XRD patterns of Orientated P4VP(1)$_{0.45}$ with Col$_h$ Phase

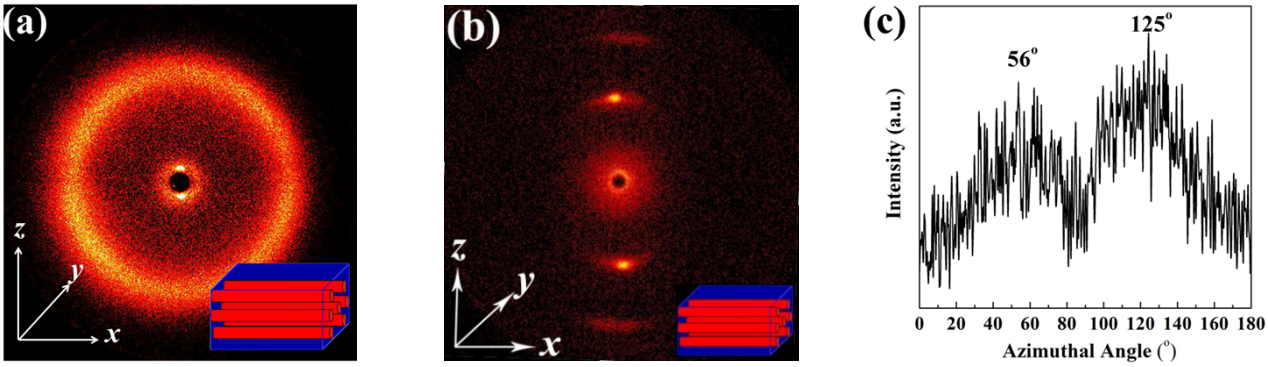

Figure S9. (a) and (b), 2D XRD patterns of P4VP(**1**)$_{0.45}$ recorded using Bruker D8 Discover and Bruker AXS (Nanostar), respectively, with the X-ray incident beam perpendicular to the shear direction. The sample was oriented by mechanical shearing. The *x*- and *z*-direction represent the shear direction and shear gradient, respectively. The low-angle diffractions of the Col$_h$ phase are located on the meridian (shear gradient), indicating that the P4VP cylinder is parallel to the shear direction. (c) Azimuthal profile of the high-angle scattering located in the 2θ range of 14~25° shown in (a). The intensity maxima locate at the azimuthal angles of 56° and 125° (the azimuthal angle 0° is on the meridian). This implies that the rodlike mesogen of molecule **1** is tilted ~55° away from the cylinder axis.

Thermal XRD results of P4VP(1)$_{0.15}$ and P4VP(1)$_{0.45}$

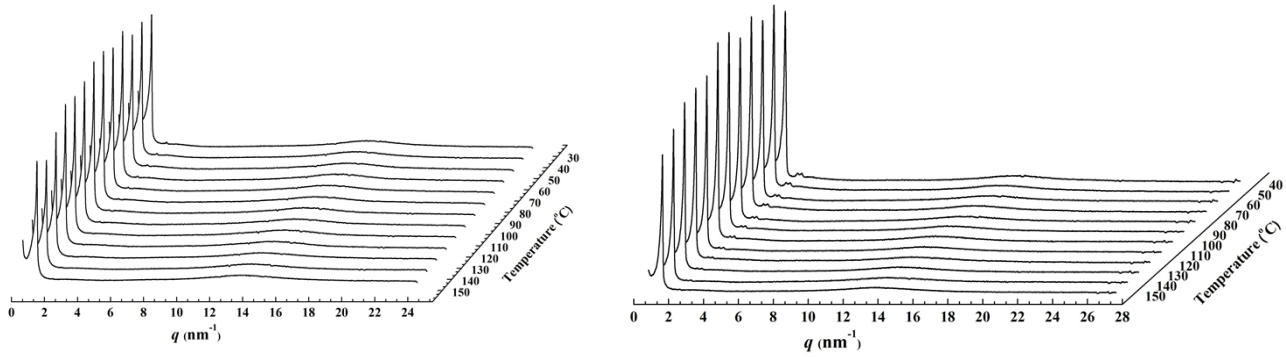

a **b**

Figure S10. 1D XRD profiles of (a) P4VP(**1**)$_{0.15}$ and (b) P4VP(**1**)$_{0.45}$ recorded upon heating to 150 °C. It is observed that the diffraction intensity starts to decrease gradually when the temperature becomes higher than the sample's glass transition temperature. As no abrupt drop of the diffraction intensity, which is associated with the order-disorder transition, is observed in the temperature range investigated. Therefore, we consider that the samples can maintain their LC structures up to 150 °C.

Reference

1. J. M. Tour, A. M. Rawlett, M. Kozaki, Y. X. Yao, R. C. Jagessar, S. M. Dirk, D. W. Price, M. A.

Reed, C. W. Zhou, J. Chen, W. Y. Wang and I. Campbell, *Chem-Eur J*, 2001, **7**, 5118.

2. S. Yagai, S. Mahesh, Y. Kikkawa, K. Unoike, T. Karatsu, A. Kitamura and A. Ajayaghosh, *Angew Chem Int Ed*, 2008, **47**, 4691.

3. G. Z. Liu and J. J. Gooding, *Langmuir*, 2006, **22**, 7421.

4. A. P. Melissaris and M. H. Litt, *J Org Chem*, 1992, **57**, 6998.

5. J. F. Zheng, X. Liu, X. F. Chen, X. K. Ren, S. Yang and E. Q. Chen, *ACS Macro Letters*, 2012, **1**, 641.

6. G. Ten Brinke, J. Ruokolainen and O. Ikkala, *Europhys. Lett.*, 1996, **35**, 91.